FP7-600716

Whole-Body Compliant Dynamical Contacts in Cognitive Humanoids

D2.2
Models of human whole body motions in contact with rigid and compliant support surfaces

Editor(s)	Morteza Azad[1], Michael Mistry[1] and Jan Babič[2]
Responsible Partner	JSI
Affiliations	[1] School of Computer Science, University of Birmingham, UK. [2] Department for Automation, Biocybernetics and Robotics, Jožef Stefan Institute, Ljubljana, Slovenia.

Status-Version:	Final-1.0
Date:	29/2/2016
EC Distribution:	Consortium
Project Number:	600716
Project Title:	Whole-Body Compliant Dynamical Contacts in Cognitive Humanoids

Title of Deliverable:	Models of human whole body motions in contact with rigid and compliant support surfaces
Date of delivery to the EC:	29/2/2016

Workpackage responsible for the Deliverable	WP2
Editor(s):	Morteza Azad, Michael Mistry and Jan Babič
Contributor(s):	Morteza Azad (UB), Michael Mistry (UB), Chie Takahashi (UB), Elmar Rueckert (TUD), Jan Peters (TUD), Jernej Čamernik (JSI), Jan Babič (JSI)
Reviewer(s):	
Approved by:	All Partners

Abstract	The scope of the current deliverable is to present the results on developing models of human whole body motions in contact with environment.
Keyword List:	contacts, model learning, probabilistic movement representations

Document Revision History

Version	Date	Description	Author
v. 1.0	29 Feb 2016	Final Version	Morteza Azad

Table of Contents

Chapter 1

Introduction

This deliverable summarizes the contribution of the CoDyCo consortium in tasks T2.2 and T2.3 at the end of the third year. These tasks are *design of models for human whole body motion in contact*, and *strategies of dealing with uncertainties in contact*, respectively. The results are briefly explained in four chapters. In chapter 2, dynamic manipulability of the centre of mass (CoM) is introduced as a metric for measuring the balance ability of legged robots while they are in contact with their environment. Experiments on human subjects show the applicability of this theory in analysing balancing recovery motion in humans. Chapter 3 investigates the use of supporting contact (and its relationship with task) while it is required for accomplishing a task. In the experiments, human subjects are asked to reach a target by the motion of one arm while they has to maintain their postural balance with the other arm. In a novel movement model, strong correlations between both arms are found which were used to predict the reaching motion solely from observing the motion related to keeping postural stability. This finding has the potential to impact pre-tests of central nervous system disorders that are less prone to factors like stress, sleep deprivation and age compared to the classical cognitive tests. In robotics, the model can be exploited to overcome current limitations of autonomous robots in interacting with the environment through supportive contacts. In chapter 4, the effects of using handles is studied for posture control of standing subjects while they are perturbed by external forces. It is shown that the use of handles significantly reduces the displacement of the centre of pressure. Also, it is observed that subjects clearly relied on using the handle for support, even though the perturbations did not pose a significant balance threat. Chapter 5 is a report of pilot study on learning compliant contacts by human subjects. Subjects are asked to push a complaint surface to a certain target in order to learn the parameters of the contact. The compliant surface is realized by using a haptic device. Then, in a trial experiment, the performance of the subjects is analysed in reaching a new target position in terms of the time needed to reach that target.

Chapter 2

Manipulability of the Center of Mass: A Tool to Study, Analyse and Measure the Ability to Balance

This chapter introduces a set of metrics to study, analyse and measure the ability to balance for both humans and legged robots. This set of metrics, which we call manipulability of the center of mass, are defined based on the concept of end-effector manipulability in the literature. Regarding the center of mass as an end-effector and using impulsive dynamics, the metrics are calculated to study the ability to move and accelerate this point. They graphically show the instantaneous change of the center of mass velocity due to the unit weighted norm of instantaneous changes of the joint velocities or impulses at the joints. The proposed metrics can be computed for humans and general legged robots with floating base and multiple contacts with the environment in 3D space. This chapter also provides the results of experiments on humans to verify the application of the metrics. In the experiments, the centers of mass of human subjects in different configurations are perturbed and joint torques are computed by using inverse dynamics. The metrics are shown to be suitable for comparing different postures in the sense of the total required effort for balance maintenance.

Further details are in the confidential appendix.

Chapter 3

Postural Control Precedes and Predicts Volitional Motor Control

Supportive hand contacts are essential for mastering every-day life tasks, for example, when reaching for a glass on the highest shelf humans typically have to use the other hand to support their body on the kitchen table. In such scenarios, the motion of the body and both arms have to be perfectly synchronized to successfully perform the reaching motion and to simultaneously ensure the postural stability. However, little is known about the underlying processes that govern the motion of the human body during and after the learning of these kinds of concurrent motor skills. To study the effect of supportive contacts on motor control of reaching, an innovative full-body experimental paradigm was established that extends current experimental methods to a more ecological setting. The task of the subjects was to reach with their right arm for a distant target on a screen while postural stability could only be maintained by establishing an additional supportive hand contact with their left arm. To examine adaptation, non-trivial postural perturbations of the subjects' support base were systematically introduced. A novel probabilistic trajectory model approach was employed to analyze the correlation between the motions of both arms. We found that subjects adapted to the perturbations by establishing supportive hand contacts that were dependent on the location of the reaching target. Moreover we found that the trunk motion adapted significantly faster than the motion of the arms. However, the most striking finding was that observations of the initial phase of the left arm or trunk motion (100-400 ms) were sufficient to faithfully predict the complete movement of the right arm. Overall, our results suggest that the goal-directed arm movements determine the supportive arm motions that ensure postural stability and that adaptation happens on different time scales, where the motion of heavy body parts adapts faster than light arms.

The details are in the confidential appendix.

Chapter 4

Use of rigid contacts during continuous perturbations

Standing balance in human everyday environment is often exposed to unpredictable and continuous external perturbations. Moreover, when postural control is impaired or challenged, handrails, canes, and handles are often used to assist maintaining balance and the effects of these firm supportive contacts in such conditions should be considered. Therefore, we examined changes in postural control in response to continuous, unpredictable perturbations and explored the effect of using a handle as a supportive contact. Postural control of standing subjects was assessed with measurements of centre of pressure (COP), which we also compared with perturbation waveform and forces exerted on the handle, to check for correlations. Kinematic data were used to determine changes in posture and electromyographic data to define the magnitude of muscle activity. The use of handle affected the control of posture by reducing the excursions of COP. The reduction was found to be more reflective in the posterior direction of COP excursions and was also in line with higher forces exerted on the handle in the same direction. The change of posture was immediate when the contact to the handle was omitted and significantly different between the two conditions. Muscle activation levels of the trunk flexor were significantly higher in the hand supported trial. In summary, we found that subjects clearly relied on using the handle for support, even though the perturbations did not pose a significant balance threat. Results of direction specific control of posture with hand support can be considered in rehabilitation and fall prevention programmes.

1 Introduction

Postural control is one of the vastly investigated area of human motor control in the last few decades. Most of the research on postural control focused on the role of sensory input in maintaining postural control during quiet standing, and in response to external balance perturbations. However, in our daily lives handrails, canes and handles are often used to assist maintaining balance, since they provide additional supportive contacts with the environment. With respect to the use of hand contacts for postural control, one of the most investigated phenomena is "light touch" [8, 12]. These light, fingertip contacts with stationary objects provide an additional sensory input, which helps individuals to better position them in space [8].

Furthermore, a more accurate sensory information improves postural control by reducing the amplitude of the centre of pressure (COP) movement [8, 9, 10, 17]. However, hand contacts can serve as more than just sensory input. In situations where balance is exposed to larger perturbations, such as experienced on a moving bus or train, a firm hand contact (i.e. holding) is needed, as it provides a much better stabilising potential than a light touch [13]. Holding to a handle, besides increasing the base of support of a standing individual, also enables generation of forces at the hand to counteract such perturbations [16, 1]. For this, the location of the handle with respect to the subjects position is important. Babi et al. [1] recently found that handle position relative to the subject, along with support surface perturbation direction and intensity, has a significant effect on the maximal forces exerted at the handle during support surface perturbations in quiet standing. More specifically, lower forces exerted at handles located at shoulder and eye level were needed to maintain a comparable peak displacement of the COP. This indicates that handles were used for postural control irrespective of their position, but certain handle positions could be exploited more efficiently. Previously mentioned studies all based on discrete perturbations of balance. Such perturbations evoke reactive postural responses and conclusions were made on the basis of these responses. However, a major component of such responses is comprised of motor actions that are related to various sensorimotor reflexes and in less extent to the voluntary component of the postural control [13]. In contrast to discrete perturbations, continuous perturbations involve both reactive and proactive components of motor actions and in this sense offer a complementary insight into the postural control. Therefore, in this research we focused on changes in postural control during continuous perturbations of subject's balance. We aimed to record the mechanical function of the arm in a function of whole body balance stabilization to measure the effect of a firm hand contact on postural control.

2 Methods

We measured thirteen healthy right-handed young adults (average age = 22.2 years, SD = 2.2 years, average height 179 cm, SD = 6.2 cm and average weight = 76.7 kg, SD = 8.4 kg). The study was previously approved by the National medical ethics committee (No. 112/06/13) and all subjects participated after giving their written consent. Data of three subjects were excluded from the analyses due to some technical issues.

2.1 Experimental protocol

Subjects were standing on a force plate while their standing balance was being perturbed for 5 minutes by a motorized waist-pull system [14] (Fig 1). They were required to keep upright with their feet placed at hip width, look straight ahead, and maintain balance without making any unnecessary corrective steps. The experiment consisted of two conditions: balancing with ("with handle"; WH) and without ("no handle"; NH) holding onto a handle. In the WH condition subject held onto a stationary handle (diameter = 3.2 cm, length = 12 cm) positioned at shoulder height [1] with their right hand. In the NH condition subjects were standing freely with their arms folded across their chest. Balance was perturbed using a random white noise signal constructed to emulate mild, daily life perturbations (e.g., public transport) bus and

avoid large, abrupt, and startling balance perturbations. This perturbation signal was based on pilot experiments, had a frequency range between 0.25 and 1.00 Hz and the maximum perturbation force of 11% of the subject's body weight. Kinetic data were collected using a force plate (9281CA, Kistler Instrumente AG, Winterthur, Switzerland) under the subjects feet and a 3-axis force sensor (45E15A, JR3, Woodland, USA) on the base of the handle, both at 1000 samples/s. Unilateral (right hand side) kinematic data were collected at a sampling rate of 100 samples/s using a contactless motion capture system (3D Investigator, Northern Digital Inc., Waterloo, Ont., Canada) consisting of a 3×3 camera array. Seven active markers were attached on the subject's right 5th metatarsal-phalangeal, ankle, knee, hip, shoulder, elbow and wrist joint. Electromyographical (EMG) activity of the right leg (Tibialis Anterior; TA, Gastrocnemius lateralis: GA) and of the trunk (Multifidus; MF, Obliques Externus; OE) was measured using Biometrics DataLOG MW8X at a sampling rate of 1000 samples/s. Before the start of the experiment, subjects performed three maximal voluntary contractions (MVC) of each of the measured muscles and were exposed to 14 trials of 5 minutes of the WH condition. The aim of these preparatory WH trials was to familiarize the subjects with the experimental set-up and avoid any learning effects observed in previous balance experiments.

2.2 Data analysis

Anteroposterior displacement of the subjects centre of pressure (COP) was calculated from the data provided by the force plate on which the subjects were standing. Kinematic data were low pass filtered (zero lag, 2nd order Butterworth algorithm, cut-off frequency 20 Hz) [2] and ankle, knee, and hip joint angles were calculated from the joint markers coordinates. Mean values of joint angles over time were fitted using an exponential model $y = A^{e-t/\tau} + C$, where A is the gain of the exponential process, τ is the time constant, C is the offset, and t refers to the trial number) to describe evaluation of motor adaptation over time [6]. The onset of reaching a plateau (adaptation stabilized) was defined by calculating point in time at the three time constants (3τ) of the fitted exponential curve. This is the point when the function reaches a value of less than 5% of its starting value and was considered as the adaptation stabilized. EMG was band-pass filtered (zero lag, 2nd order Butterworth algorithm, with cut-off frequencies of 20 and 450 Hz), full-wave rectified and normalized by division with the MVCs. By applying a low pass filter (zero lag, 2nd order Butterworth algorithm, 10 Hz cut-off frequency), we created envelopes of EMG signals and then integrated them over time, to observe the accumulated EMG activity.

2.3 Statistical analysis

To compare the NH and WH conditions we calculated the average COP displacement, hip, knee, and ankle angles and contact forces exerted on the handle over the 5 minutes for each subject. These individual average values were used for statistical analysis. We used paired samples t-test analysis to investigate the differences between the WH and NH conditions and linear correlation to investigate the relationship between the COP displacement and the magnitude of the perturbation (separately for anterior and posterior directions) and between COP and the exerted handle contact force. All statistical analyses were performed using SPSS

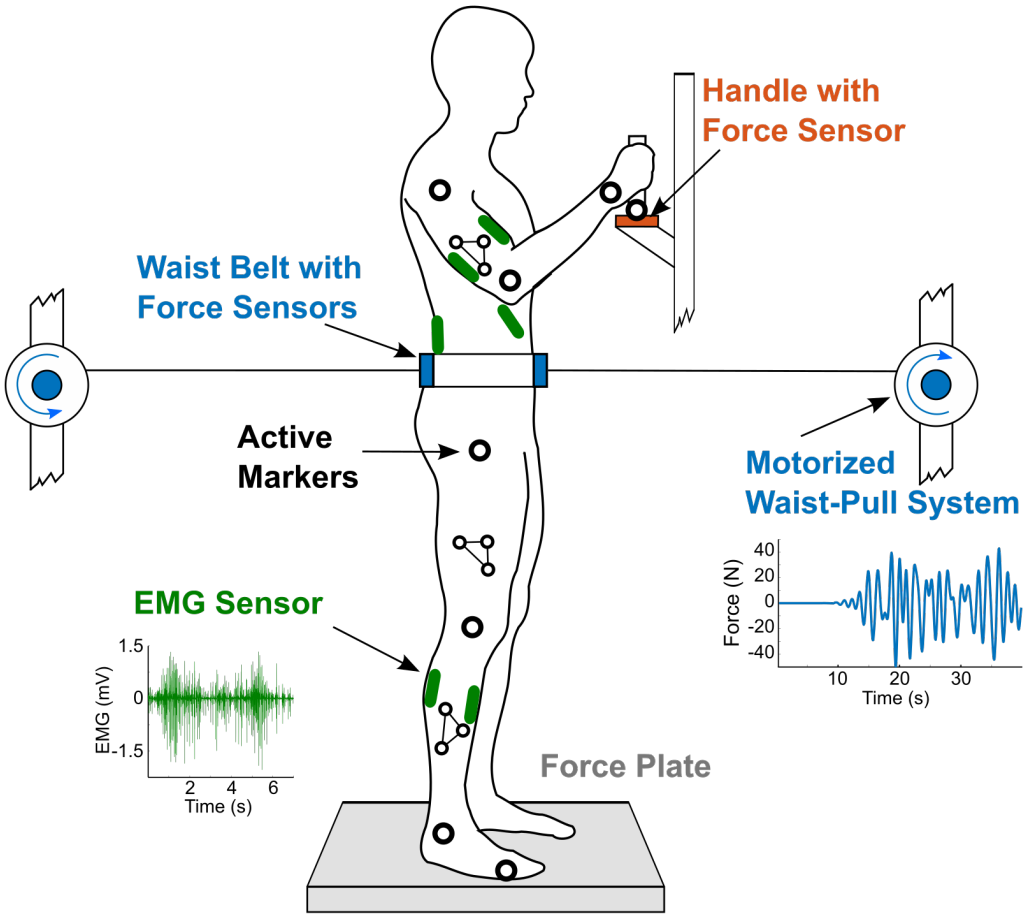

Figure 1: **Experimental setup.** The subject is standing on a force plate, wearing a waist belt connected to the motorized waist-pull system which generated translational force perturbations in the anterior-posterior direction using a random white noise signal constructed to emulate mild, daily life perturbations. The actual perturbation waveform is shown on the plot below the motorized waist-pull system.

21 Inc., Chicago, USA and statistical significance was set at $\alpha = 0.05$. The effect size (d) was calculated by using standard Cohens equation ($\hat{d} = \frac{\bar{X}_1 - \bar{X}_2}{s}$) [4].

After comparing the two trials we checked for direction specific differences of COP displacement within each trial. For this, we used a paired samples t-test on averaged measures of anteroposterior COP displacement. The relationship between the perturbation and the COP displacement was investigated in more detail by correlating the perturbation force and COP displacement and by correlating perturbation force and forces on the handle.

3 Results

Average anteroposterior displacements of the COP during the NH and WH conditions are shown in Fig 2. In both conditions COP displacement was larger in the anterior direction (mean ± SE: NH 38.45 ± 1.6 mm, WH 18.15 ± 1.2 mm) compared to posterior (mean ±

SE: NH -34.88 ± 2 mm, WH -11.02 ± 1.5 mm), but this difference was significant only for the WH condition ($t(9) = 2.81$, $p = .02$, $d = 1.52$). Hence, the remainder of our COP analyses were conducted for the anterior and posterior directions separately.

Overall, COP displacements were significantly larger in the NH condition compared to WH condition, both in the anterior (difference of 20.3 mm, $t(9) = 7.78$, $p = .001$, $d = -4.15$) and posterior direction (difference of 23.9 mm, $t(9) = -11.09$, $p = .001$, $d = -3.8$).

As can be seen from Fig 3A, the correlation between the COP displacement and perturbation force was $r_p = .77$ ($p < .001$) and $r_a = .82$ ($p < .001$) in the NH condition for the posterior and anterior direction, respectively. For the WH condition (Fig 3B) the correlations were $r_p = .67$ ($p < .001$) and $r_a = .89$ ($p < .001$) for the posterior and anterior direction, respectively.

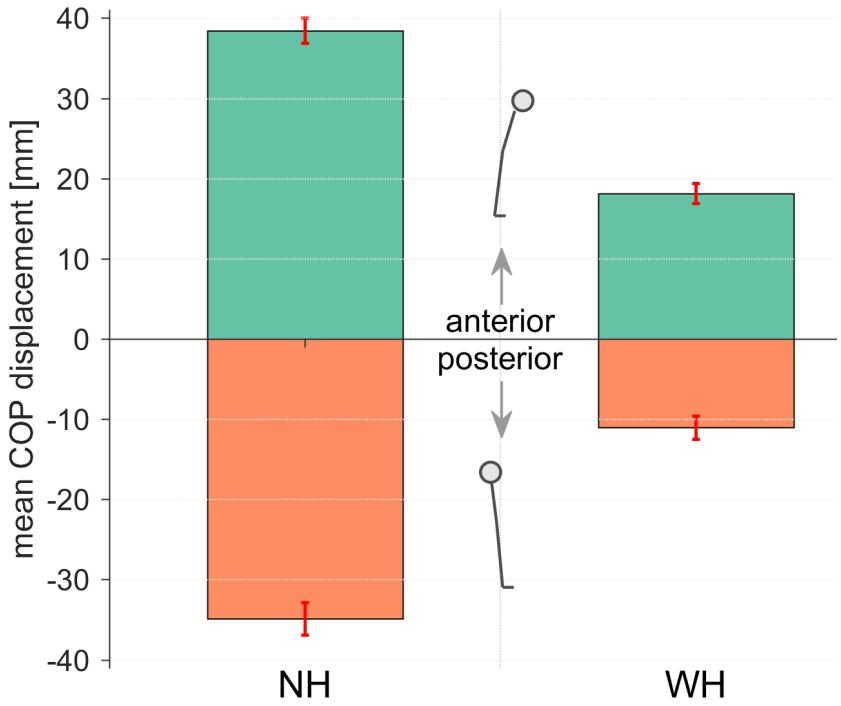

Figure 2: **Anteroposterior displacement of COP.** Mean COP displacement in NH and WH trials, for the anterior (positive) and posterior (negative) directions. Error bars indicate $\pm$ 1 standard error of the mean.

Correlations between the forces exerted on the handle and the perturbation force (Fig 3C) were large in both anterior ($r_p = .85$, $p < .001$) and posterior direction ($r_a = .81$, $p < .001$). However, the slope of a least-squares linear fit to the data indicates, that subjects utilized the handle considerably more for perturbations in the posterior direction ($k_p = 1.3$) than for perturbations in the anterior direction ($k_a = .86$).

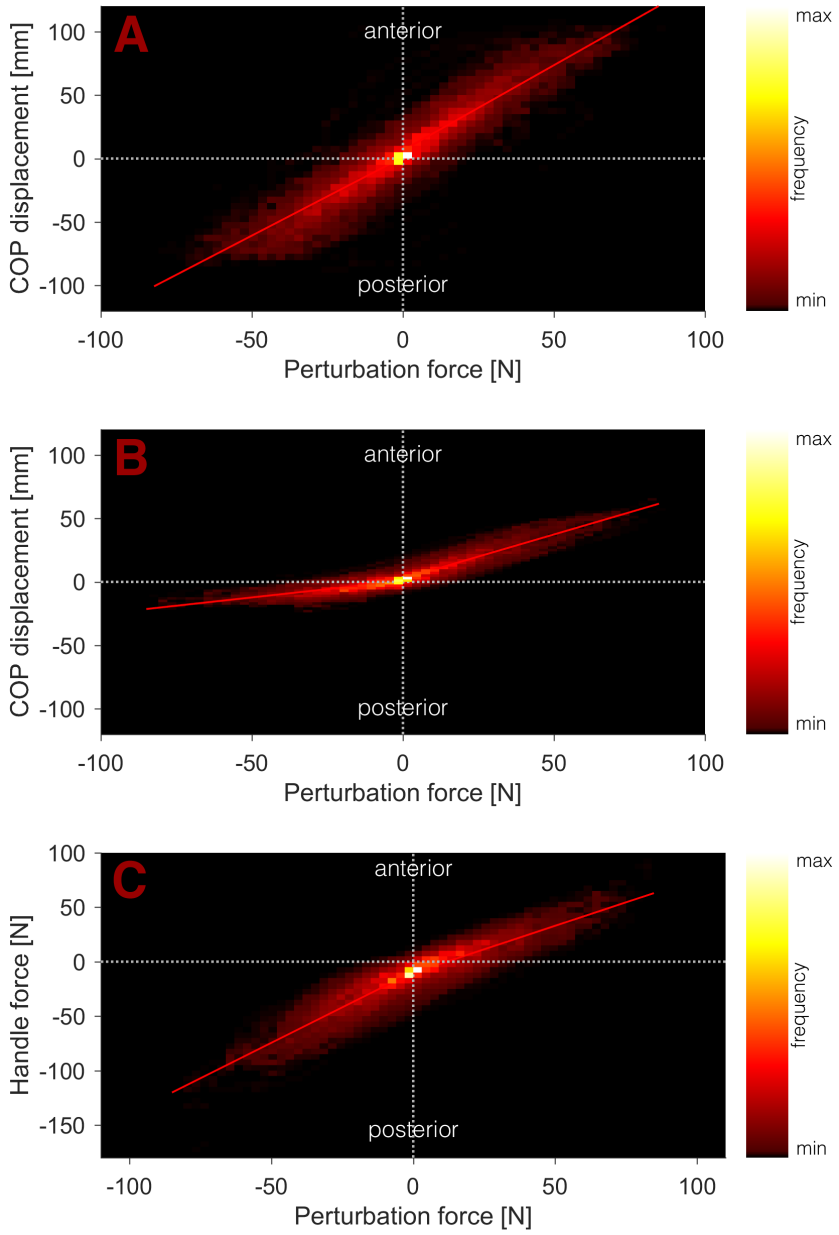

Figure 3: **Correlation. (A)** Correlation between the perturbation force and COP displacement in the NH condition, **(B)** correlation between COP displacement and perturbation force in the WH condition, and **(C)** correlation between handle force and perturbation force in the WH condition. All correlations were calculated separately for the anterior (positive) and posterior (negative) direction.

Joint angles prior to the start of perturbation were significantly smaller in the NH condition compared to WH condition (Fig 4). Differences were the largest in the knee (mean $\pm$ SE: 169.4 $\pm$ 1.4° for NH, 172.9 $\pm$ 1.4° for WH, $t(9) = -4.05$, $p = .01$, $d = 1.36$), followed by the hip (mean $\pm$ SE: 179 $\pm$ 1.8° for NH, 181.6 $\pm$ 1.5° WH, $t(9) = -2.95$, $p = .024$, $d = 1.13$), and ankle (mean $\pm$ SE: 110.4 $\pm$ 1.1° for NH, 112.1 $\pm$ 1.2° WH, $t(9) = -2.71$, $p = .038$, $d = 1.08$).

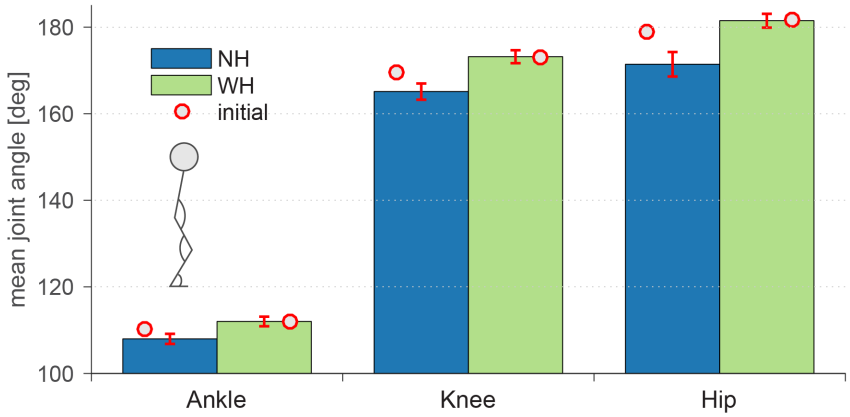

Figure 4: **Ankle, knee and hip joint angles.** Mean value of joint angles during the perturbation is given for NH (blue bars) and WH condition (green bars) and mean joint angles prior to the start of perturbation are shown as red circles above bars. Error bars indicate $\pm$ 1 standard error of the mean.

Ankle (A), knee (B), and hip (C) angles over the time course of the perturbation are shown in Fig 5. Exponential curves fitted to the data show that mean joint angles in the NH condition changed after the perturbation onset before reaching a steady state. The steady state was reached first by the ankle angle (86 s after perturbation onset), followed by the knee angle (112 s after the perturbation onset) and finally hip angle (195 s after the perturbation onset), resulting in more ankle, knee and hip flexion.

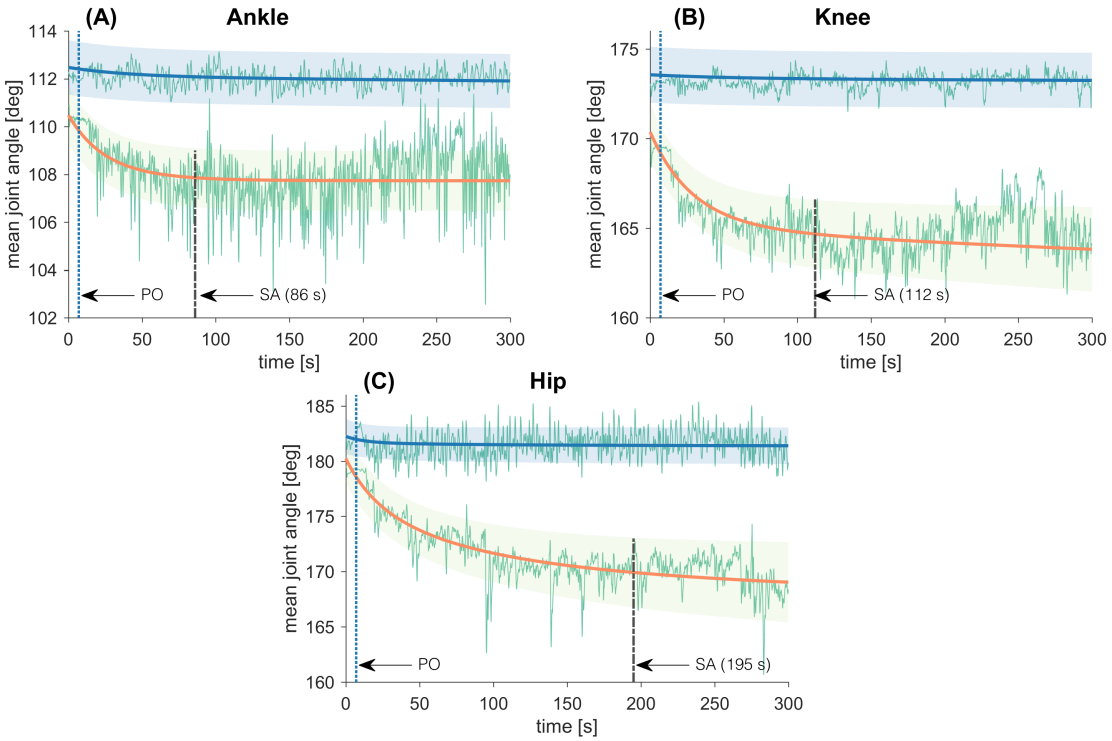

Figure 5: **Ankle, knee and hip joint angles.** Figures represent mean ankle **(A)**, knee **(B)**, and hip **(C)** angles over the time course of the perturbation. Thin solid curves represent mean joint angles during NH and WH conditions. Thick solid lines represent exponential curve fit, denoting adaptation of joint angles in the NH (orange) and WH (blue) conditions, while shaded areas represent standard error of the mean. The dotted vertical lines represent perturbation onset (PO) while the dashed vertical lines indicate stabilized changes (adaptation) in the joint angles (SA).

Finally, muscle activity is significantly lower during the WH condition than during the NH condition both for the leg muscles (GA $t(9) = 3.57$, $p = .04$, $d = -0.89$; TA $t(9) = 6.41$, $p = .002$, $d = -1.85$) and trunk muscle (MF $t(9) = 6.5$, $p = .001$, $d = -1.01$), as can be seen in Fig 6. Leg muscle activity is lower for 18.4 $\pm$ 4.9% in the GA (mean $\pm$ SE: NH: 28.97 $\pm$ 6.5% MVC, WH: 10.6 $\pm$ 2.3% MVC) and for 23.7 $\pm$ 3.5% in the TA (mean $\pm$ SE: NH: 27.21 $\pm$ 4% MVC, WH: 3.47 $\pm$ 1.9%), while trunk muscle activity is lower for 14.3 $\pm$ 2.1% in the MF (mean $\pm$ SE: NH: 36.17 $\pm$ 4.5% MVC, WH: 21.83 $\pm$ 3.7%).

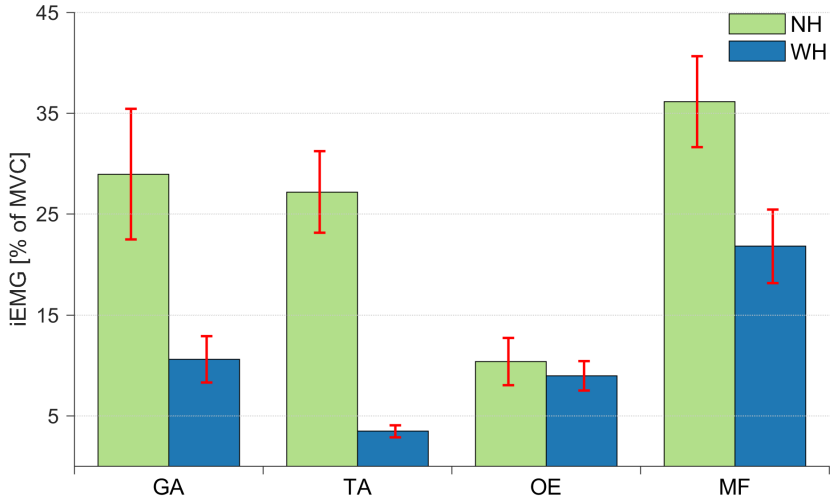

Figure 6: **Muscle activity.** Mean integrated EMG activity of leg (GA and TA) and trunk (OE and MF) muscles during the NH (green bars) and WH condition (blue bars). Error bars indicate $\pm$ 1 standard error of the mean.

4 Conclusions

Standing balance in human everyday environment is often exposed to unpredictable and continuous external perturbations. Moreover, when postural control is impaired or challenged, handrails, canes, and handles are often used to assist maintaining balance and the effects of these firm supportive contacts in such conditions should be considered. Therefore, we examined changes in postural control in response to continuous, unpredictable perturbations and explored the effect of using a handle as a supportive contact. Postural control of standing subjects was assessed with measurements of centre of pressure, which we also compared with perturbation waveform and forces exerted on the handle, to check for correlations. Kinematic data were used to determine changes in posture and electromyographic data to define the magnitude of muscle activity. COP displacement, hip, knee, and ankle angles, leg and trunk muscle activity and handle contact forces were analysed for the anterior and posterior directions separately, as COP displacement was significantly larger in the anterior direction (WH, 7 mm, $p = .02$). Perturbation force was strongly correlated to COP displacement (all $r > .65$) and handle forces ($r > .8$) in both directions. COP displacement was significantly larger in the NH condition compared to WH condition (anterior: 20 mm, posterior: 24 mm, both p

$= .001$) and regression indicated that subjects utilized the handle slightly more for posterior perturbations. In the NH condition, all joint angles decreased in anticipation of the perturbation (2-4°, all $p < .04$) and until 86-195 s following perturbation onset. Finally, leg (18-24%) and one of the trunk (14%) muscles increased their activity in the NH condition (all $p \leqslant .04$). In summary, we found that subjects clearly relied on using the handle for support, even though the perturbations did not pose a significant balance threat. Results of direction specific control of posture with hand support can be considered in rehabilitation and fall prevention programs.

Chapter 5

Learning compliant contacts

A pilot study aims at examining how humans learn compliant force dynamics and modulate their whole-body motions to reach anticipated goals. Here, we present an experimental idea to measure the goal-directed movements against compliant forces, and then illustrate the ongoing results which were conducted for a few human subjects. At this pilot stage, we are focusing on the simple linear compliant case and discuss further experiments. To deepen understanding of the mechanism in humans, it would be beneficial to develop the humanoid robot control in interacting with multiple compliant surfaces.

1 Introduction

Humans can learn how to control their own body movements in an uncertain environment, and utilise it to predict the consequences of actions and to achieve a behavioural goal [18, 5]. A considerable amount of research has shown the human capabilities of generalization in visuo-motor learning and has been exploring the underlying mechanisms [7, 11]. A certain exposure to a new physical environment facilitates to generalize the spatial and temporal characteristics of the point-to-point movements via error-based learning and perturbation paradigm. In the real-world interactions, there are varied and complicated force dynamics (i.e., governed by not only simple linear principles) when making a contact with an object and handling it. The optimal functions seem to be perceptually learned via repetitive movements against the force. However, to our knowledge, little is still known about how humans can generalize the compliant force dynamics itself and utilize it to their future motor plan.

The CoDyCo project has been investigating the whole-body coordination mechanisms in arm reaching movements and the postural balance control in assistive contact with rigid and/or compliant surfaces. Like humans, robots are required to flexibly adjust their posture and to coordinate the physical mobility with augmented autonomy. We expect that humans could generalize the force principles in a cognitively robust way via force-feedback from the early stage of the body movements. To explore the generalization mechanism of the force dynamics in humans and to model it would provide a useful strategy in humanoid robot control. The successful model could be exploited to effectively control autonomous robots' whole-body balance in interacting with the environment through supportive contacts.

In a pilot study, we focused on a simple case: linear compliant force. We employed a haptic device, Haptic Master (Moog, Inc.), which is controlled by a set of a computer programmes

to render robotic manipulandum for force feedback. The pilot experiment measured the end-effector movements controlled by human subjects and analysed the dynamic properties of the movements against the compliant force and the performance.

2 Methods

2.1 Modelling

In general, spring-damper force ($\mathbf{F}$) is formulated by the position and the velocity with parameters: spring stiffness (k) and spring damping factor (λ). Here, it is simplified for one direction ($\mathbf{Z}$).

$$\mathbf{F} = k\mathbf{Z}^n + (\lambda\mathbf{Z}^p)\dot{\mathbf{Z}}\,. \tag{1}$$

We employed the ready-made spring model in the Haptic API, where the compliant force formula was assigned to the device, the Haptic Master. The compliant force was rendered by the end-effector position and the velocity with the parameters in real-time (Fig. 1).

2.2 Experimental Design

As a pilot study, we employed a simple linear spring-damper formula:

$$\mathbf{F} = k\mathbf{Z} + \lambda\dot{\mathbf{Z}}\,. \tag{2}$$

The compliant force formula is assigned to the model in the Haptic Master. Aiming to simplify analysing the performance, the forces and the movements were constrained in the only one direction, here, in the vertical (Z) direction to the ground.

Human subjects learned a spring compliant force via repetitive reaching Bmovements to the first target (z = t1) in a certain period of time, - so called "Learning session". Then, they were asked to move the end-effector to the second, or test, target (z = t2), which was set more far from the t1 position, as a test trial; so, more force would be required for this movement (Fig.2). In order to achieve the t2 target, the participants would exploit their prior knowledge of the force dynamics experienced via learning session. We will evaluate whether and how the motion performance is likely to follow the formula previously learned.

2.3 Apparatus and Stimuli

The haptic device, "Haptic Master" consisted of a large robotic rod with an end-effector. The "Home" position, where was the centre of the end effector is z = 0 at the workspace, was 110 cm from the ground. The spring position was set at z = 0. In this study, the rod movements were restricted in the vertical direction only.

The visual information about the task was provided at the computer display to human subjects. The computer screen was located at the right side of the Haptic Master from the subjects; where the centre of the screen was approximately 80 cm from the centre of the robotic rod. The screen was approximately 1 m away from the participants' standpoint, and 80 cm away from the centre of the end effector position. The screen displayed the target position and the end-effector position in real-time (Fig. 3). The target positions were set at z = t1 (50 mm for learning), and z = t2 (100 mm for test).

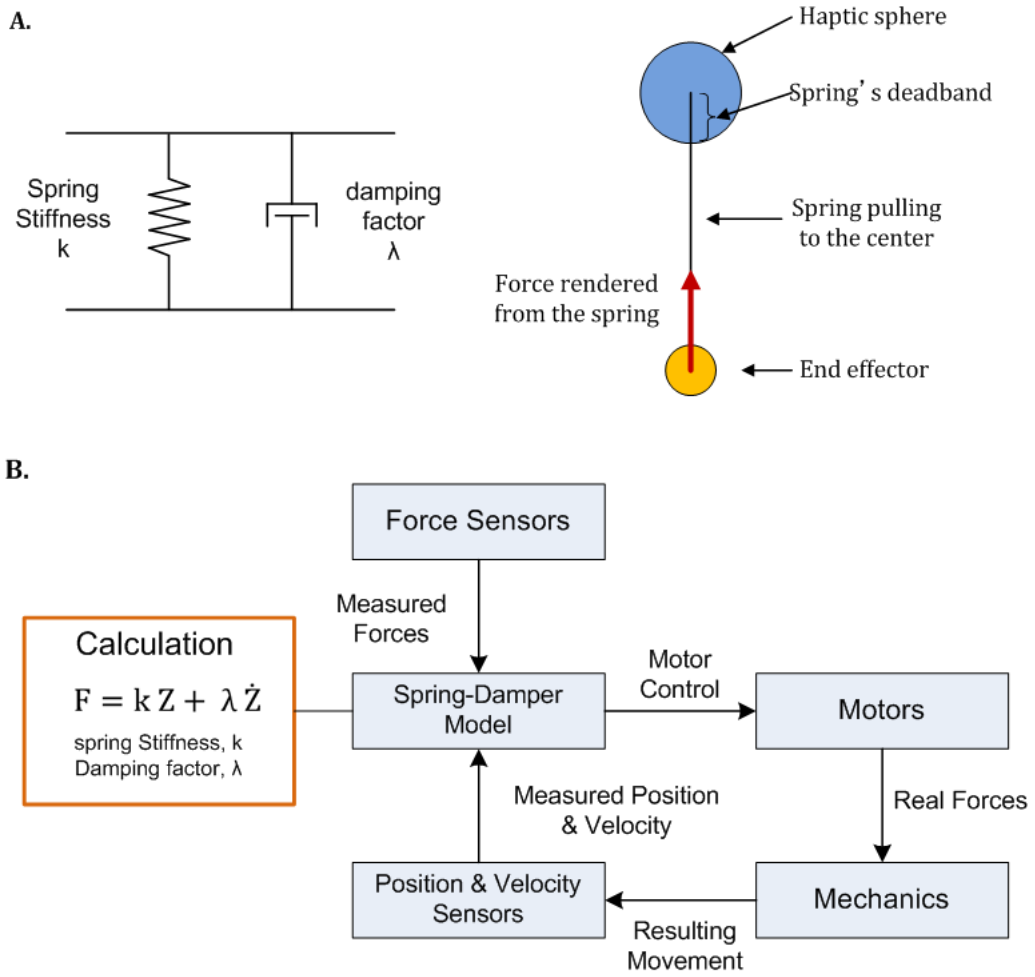

Figure 1: A. The ready-made spring model in the Haptic API. B. Block diagram of the compliant force control. The force is rendering based on the end-effector position and the velocity with parameters (spring stiffness and damping factors) in the real time.

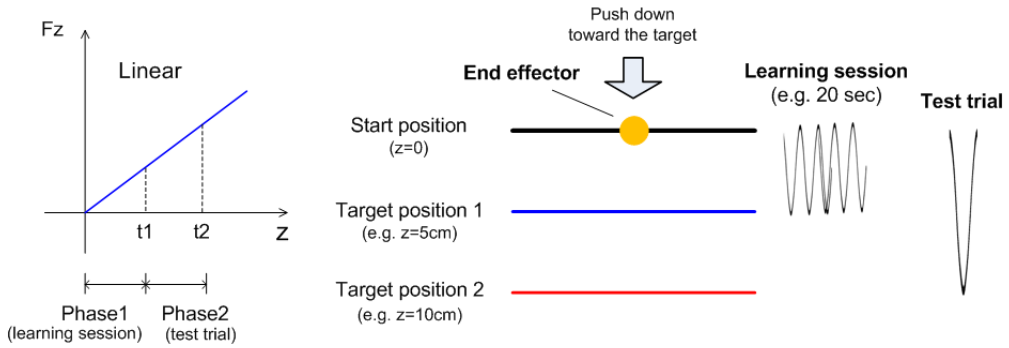

Figure 2: Experimental Design. Two target positions were set: z = t1 for learning session and z = t2 for test trial.

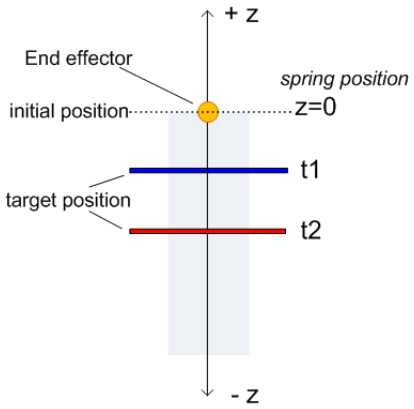

Figure 3: Experimental visual stimuli. The end-effector and the two target positions (z = t1 and z = t2) were visually indicated on the computer screen.

2.4 Procedure and analyses

Participants stood in front of the haptic device and grasped the end-effector. Firstly, they conducted a practice session followed by the main blocks. They were required to make repetitive movements against compliant force generated by the device to learn the kinetic principle. The movements were monitored by visual information on the screen. Participants pushed the end-effector to reach the target position, and then released the end-effector to allow it to freely return to the initial position (z=0). They were asked to set the centre of the end-effector position on the target as accurate as possible.

The main block consisted of two parts: Learning session and Test trial. In the Learning session, the target position was set at z= t1, described above. Participants controlled the end-effector by their own timing, or rhythm, per each movement in the current pilot study (the specific time windows were not set up by the programme for the series of movements: i.e., push the end-effector down from the start position and reach the target position). The visual feedback was given when the end-effector reached to the target; the target colour indicated this by changing from blue to yellow. Participants learnt the compliant force dynamics by the repetitive movements. he experimenter monitored the elapsed time using a stopwatch, and verbally informed the end of the session when 20 seconds passed. Participant stopped their repetitive movements immediately and prepared for the trial session.

In the Test trial, participants moved the end-effector to the target (coloured red line, z = t2) three times based on the formula they previously learned. In this phase, no visual feedback in the relationship between the end-effector position and the target was given to the subjects.

One block consists of three sets (Learning session + Test trial). Participants conducted three blocks; so, 3 blocks in total, and 9 test trials. Under the current settings, the experiment was completed within approximately 20 minutes on average.

The dynamic properties of the point-to-point movements were measured: the end-effector's position ($\mathbf{Z}$), the velocity ($\dot{\mathbf{Z}}$), and the force ($\mathbf{F}_Z$) across the time. These were recorded by the 20 msec sampling rate properties were analysed and compared between the linear and the non-linear force conditions.

3 Results and Discussions

3.1 Participants

Six male subjects (age: 28.8 +/- 3.1 (SD), height: 175.3 cm +/- 7.1 (SD), weight: 79.5 kg +/- 17.8 (SD), one left-handed) voluntarily participated in the pilot experiment. All had normal or corrected to normal vision, and they had no known motor deficits and/or any limb injuries (self-reported). They were recruited from the student and staff population at University of Birmingham. (One was not nave to the purpose of the experiment.)

3.2 Ongoing Results

The end-effector position, velocity and force were recorded. Here, illustrates the one participant's one block performance, as an example (Fig 4).

In order to examine the each reaching movement, the data were extracted from the total between the start (z = 0.01m) and the end (approx. z = t2) positions, where the end-effector was released to return to the initial position. These points were determined by calculating the each inflection point (Fig 5).

The data were averaged across three blocks; one block consisted of three (Learning + Trial) sessions; so participants ideally completed 9 sessions in total, but one (subj.03) accidentally completed only two blocks because of the setting errors. The averaged numbers of repetitions were 152.8 +/- 45.6 (SD) in the Learning session and 27.2 +/- 6.1 (SD) in the Test trial. All six participants' averaged data (the end-effector position, velocity and force) can be seen from Fig.6 to Fig. 8.

3.3 Brief Discussion

The Fig 9 showed that some participants (e.g., Subj.01, Subj.06) performed to reach the target position (z = t2) much faster than the expected time duration, which was estimated from the linear equation. That is, the t2 position was double distance of the t1 from the start position; so the reaching time would be estimated close to the double. The time would not be able to calculate by the simple linear calculation because the damping factor depends on the velocity, though.

This might be caused by the experimental design; that is, participants made the repetitive movements with their own rhythms at the learning session. Because they tend to keep their rhythms even in the consecutive trial session, and then they might have unconsciously increased the force or accelerated their speed to reach the target. This possibility can be seen at their movement profiles (Fig.7: velocity and Fig.8: force). Several studies have shown that time perception plays an important role in human motor control [3, 15]; therefore, this timing issue should be carefully considered into the experimental design and should avoid any confounding factors. To do this, we will visually guide the participants' movements with a certain time-windows in the future experiment.

Moreover, in the current pilot experiment, the judgment of reaching the target was inaccurate. Although the participants received the visual feedback at the learning session, it only indicated the end-effector crossed the target position, and also there were no task reward. The

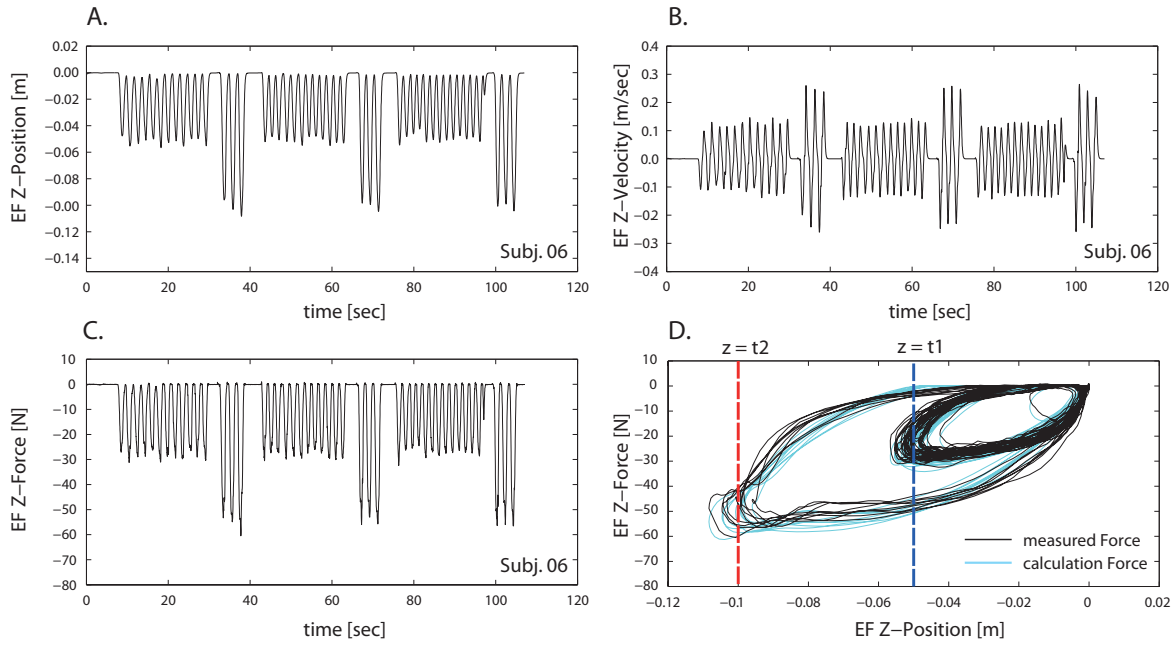

Figure 4: The total recording of the completion of the first block. (Subj. 06). **A**. End-effector Z-position, **B**. Z-velocity and **C**. Z-force. **D**. the relationship between the position and the force compared between the force directly measured by the sensor and the force calculated by the equation with the real time z-position and z-velocity.

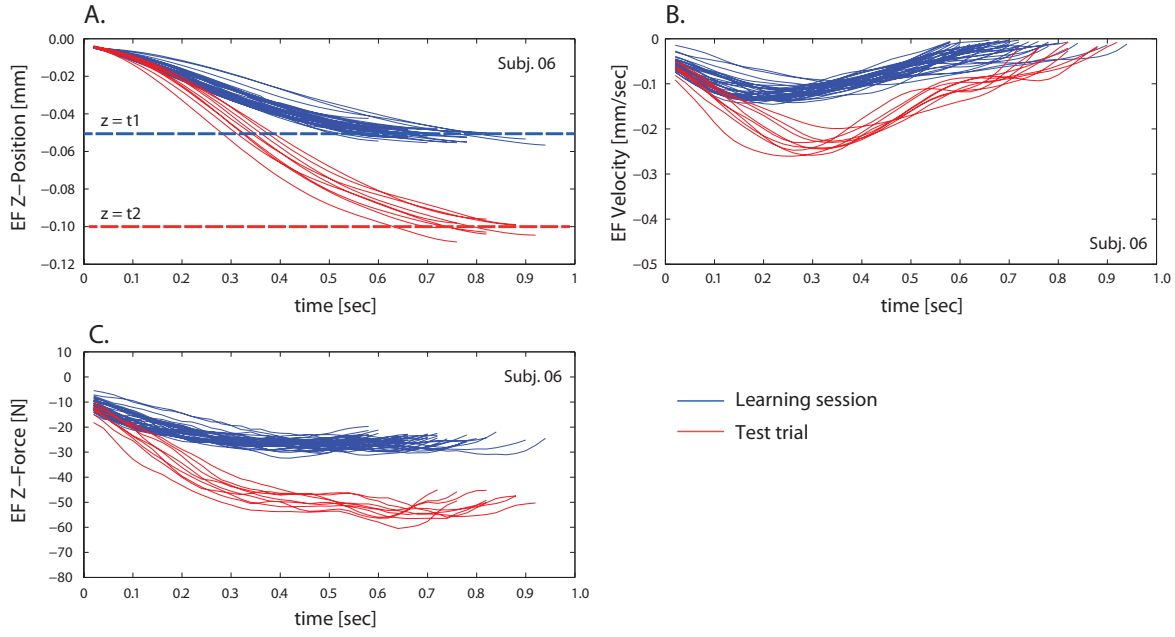

Figure 5: Experimental data for one participant (the first block, three test trials). Red lines represent the forces, which were directly measured by a sensor at the end-effector. Blue lines represent the forces, which were calculated in the real time by spring stiffness and damping factor with the end-effector position.

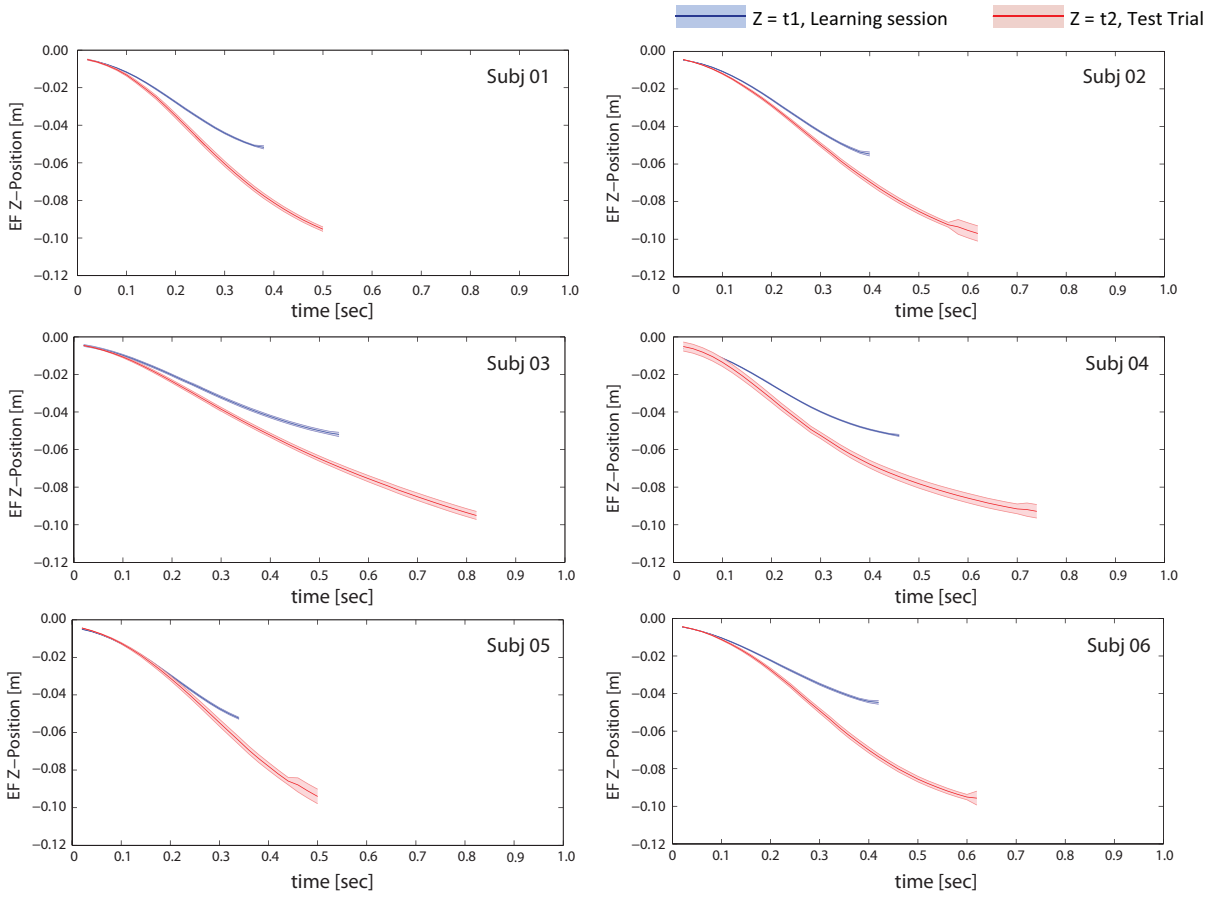

Figure 6: The averaged end-effector z-position performance in the reaching movements against the linear spring-damper force for 6 subjects. The data were averaged across 3 blocks (9 (Learning + Trial) sessions). The blue lines represent the average performance in the Learning session, and the red in the Test trial, the coloured areas represent their standard error respectively.

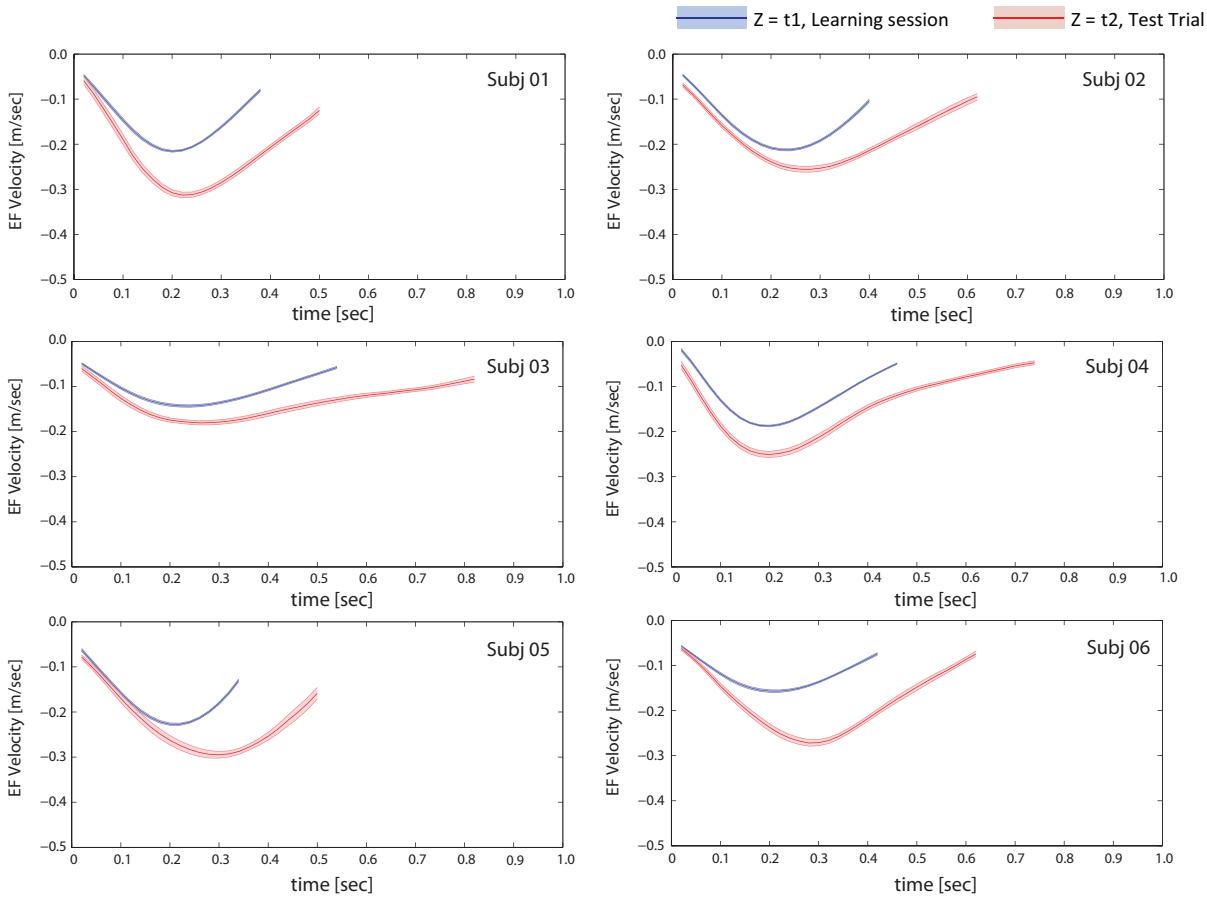

Figure 7: The averaged end-effector z-velocity performance in the reaching movements against the linear spring-damper force for 6 subjects. The data were averaged across 3 blocks (9 (Learning + Trial) sessions). The blue lines represent the average performance in the Learning session, and the red in the Test trial, the coloured areas represent their standard error respectively.

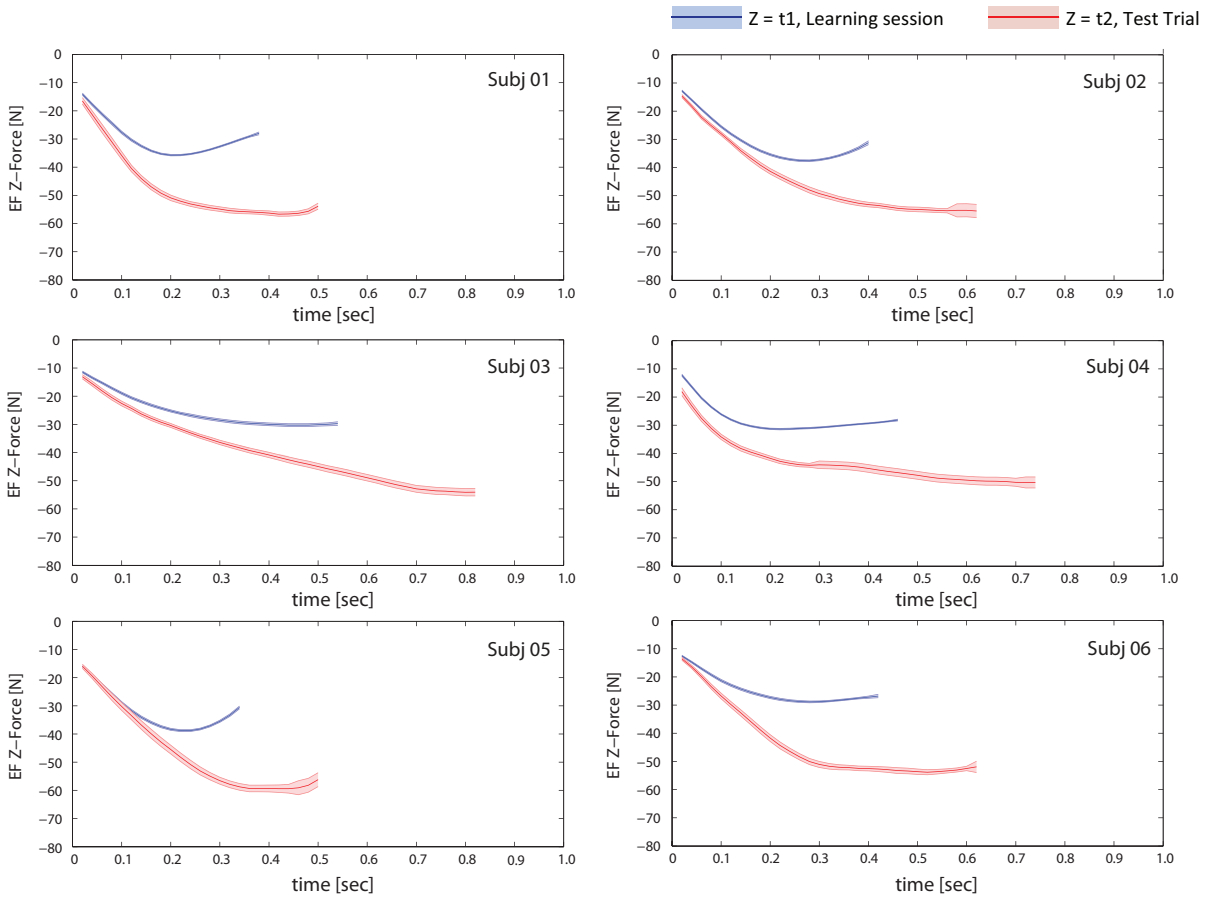

Figure 8: The averaged end-effector z-force performance in the reaching movements against the linear spring-damper force for 6 subjects. The data were averaged across 3 blocks (9 (Learning + Trial) sessions). The blue lines represent the average performance in the Learning session, and the red in the Test trial, the coloured areas represent their standard error respectively.

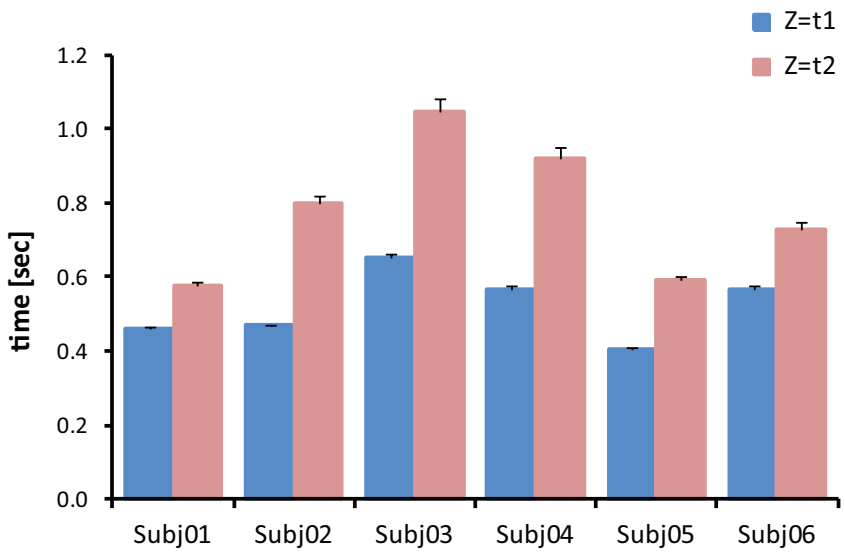

Figure 9: Illustrate averaged time to reach the targets with the comparison between the Learning session (blue) and the Test trial (red) for six subjects. The error bars represents the standard error across the total number of the repetitions.

inaccuracy would have affected their force perception and movements [15] therefore, in the next experiment, we will set a specific correct zone visually defined by a more accurate way (e.g. the similar size of sphere of the end-effector) as the target instead of the line indicators. The task completion in the Learning session would be determined by their performance and individual learning level would be evaluated by their correct movements.

The current analyses conducted for all performance in the test trial (reaching the target (z= t2) three times for each), but the performance might have needed to be evaluated focusing on the first trial only, because the first movement was directly affected by the learning session and the second and the third movements were gradually contaminated.

Overall, through the pilot experiment, we have learned the importance of the timing issue in interacting with compliant surface. We will improve the experimental design and strictly control the parameters (timing, speed, and the accuracy).

In the future experiment, based on the linear case, we will measure the pattern under the non-linear compliant forces and examine the human goal-directed performance. Besides, as well as the spring-damper, it may help the understanding of the generalization if we employ another compliant force model (e.g. object surface).

Bibliography

[1] Jan Babič, Tadej Petrič, Luka Peternel, and Nejc Šarabon. Effects of supportive hand contact on reactive postural control during support perturbations. *Gait and Posture*, 40(3):441–446, jun 2014.

[2] Roger Bartlett. *Introduction to Sports Biomechanics: Analysing Human Movement Patterns*. Routledge, Abingdon, UK, 2 edition, 2007.

[3] B Berret and F Jean. Why don't we move slower? the value of time in the neural control of action. *The Journal of Neuroscience*, 36(4):1056–1070, 2016.

[4] Jacob Cohen. *Statistical Power Analysis for the Behavioral Sciences*. Lawrence Erlbaum Associates, 2 edition, 1988.

[5] P Davidson and D Wolpert. Motor learning and prediction in a variable environment. *Current Opinion in Neurobiol*, 13(2), 2003.

[6] David W Franklin, Rieko Osu, Etienne Burdet, Mitsuo Kawato, and Theodore E Milner. Adaptation to stable and unstable dynamics achieved by combined impedance control and inverse dynamics model. *Journal of neurophysiology*, 90(5):3270–3282, 2003.

[7] S Goodbody and D Wolpert. Temporal and amplitude generalization in motor learning. *Journal of Neurophysiology*, 79(4):1825–1838, 1998.

[8] John J Jeka. Light touch contact as a balance aid. *Physical therapy*, 77(5):476–87, may 1997.

[9] Leif Johannsen, Alan M Wing, and Vassilia Hatzitaki. Effects of maintaining touch contact on predictive and reactive balance. *Journal of neurophysiology*, 97(4):2686–2695, 2007.

[10] Motoki Kouzaki and Kei Masani. Reduced postural sway during quiet standing by light touch is due to finger tactile feedback but not mechanical support. *Experimental Brain Research*, 188(1):153–158, 2008.

[11] J Krakauer, P Mazzoni, A Ghazizadeh, R Ravindran, and R Shadmehr. Generalization of motor learning depends on the history of prior action. *PLoS Biology*, 4(10):1798–1808, 2006.

[12] Vijaya Krishnamoorthy, Harm Slijper, and Mark L. Latash. Effects of different types of light touch on postural sway. *Experimental Brain Research*, 147(1):71–79, 2002.

[13] Brian E Maki and William E McIlroy. The role of limb movements in maintaining upright stance: the "change-in-support" strategy. *Physical therapy*, 77(5):488–507, may 1997.

[14] Luka Peternel and Jan Babič. Learning of compliant humanrobot interaction using full-body haptic interface. *Advanced Robotics*, 27(13):1003–1012, sep 2013.

[15] M Rank and M Di Luca. Speed/accuracy tradeoff in force perception. *Journal of Experimental Psychology: Human Perception and Performance*, 41(3):738–746, 2015.

[16] Thiago A Sarraf, Daniel S Marigold, and Stephen N Robinovitch. Maintaining standing balance by handrail grasping. *Gait & posture*, 39(1):258–64, jan 2014.

[17] Alan M Wing, Leif Johannsen, and Satoshi Endo. Light touch for balance: influence of a time-varying external driving signal. *Philosophical transactions of the Royal Society of London. Series B, Biological sciences*, 366(1581):3133–41, nov 2011.

[18] D Wolpert, J Diedrichsen, and R Flanagan. Principles of sensorimotor learning. *Nature Review Neuroscience*, 12(12):739–751, 2011.